Lactation in the Human Breast From a Fluid Dynamics Point of View

S. Negin Mortazavi
Department of Mechanical Engineering,
University of Texas at Dallas,
Richardson, TX 75080
e-mail: negin@utdallas.edu

Donna Geddes
School of Chemistry and Biochemistry,
University of Western Australia,
Crawley, Western Australia 6009, Australia
e-mail: donna.geddes@uwa.edu.au

Fatemeh Hassanipour[1]
Department of Mechanical Engineering,
University of Texas at Dallas,
Richardson, TX 75080
e-mail: fatemeh@utdallas.edu

This study is a collaborative effort among lactation specialists and fluid dynamic engineers. The paper presents clinical results for suckling pressure pattern in lactating human breast as well as a 3D computational fluid dynamics (CFD) modeling of milk flow using these clinical inputs. The investigation starts with a careful, statistically representative measurement of suckling vacuum pressure, milk flow rate, and milk intake in a group of infants. The results from clinical data show that suckling action does not occur with constant suckling rate but changes in a rhythmic manner for infants. These pressure profiles are then used as the boundary condition for the CFD study using commercial ANSYS FLUENT *software. For the geometric model of the ductal system of the human breast, this work takes advantage of a recent advance in the development of a validated phantom that has been produced as a ground truth for the imaging applications for the breast. The geometric model is introduced into CFD simulations with the aforementioned boundary conditions. The results for milk intake from the CFD simulation and clinical data were compared and cross validated. Also, the variation of milk intake versus suckling pressure are presented and analyzed. Both the clinical and CFD simulation show that the maximum milk flow rate is not related to the largest vacuum pressure or longest feeding duration indicating other factors influence the milk intake by infants.*
[DOI: 10.1115/1.4034995]

1 Introduction

Fundamental studies of transport processes in biological organs can be greatly beneficial to the understanding of the pathology of many diseases as well as addressing wider issues related to human health and wellbeing. Motivated by this basic principle, mathematical or computational fluid dynamics modeling of human organs has been applied in blood vessels [1–3], lung and respiratory system [4–6], nasal and human upper airway [7–10], liver [11–15], and brain [16–19]. These studies have found relevance in the diagnosis and treatment of diseases [20,21] as well as the development of various biomedical devices [22,23] and surgical procedures [24,25].

The female human breast is a prime example of the principle mentioned above. A wide scientific consensus points to the overwhelming advantages of breastfeeding when possible, and its long-lasting positive effects on the health of the both the infant and the mother. The prevalence of various difficulties that hinder or discourage breastfeeding is also well known among the community of experts on human lactation [26]. Also, many of the diseases of this organ are closely related to the ductal system transporting fluids, among these diseases one can name ductal blockage, breast engorgement, breast abscess, and galactocele. The investigation of the origins of breast diseases and various conventional breast conditions, as well as their diagnosis and treatment, can greatly benefit from a detailed understanding of the milk flow mechanism and the factors that influence it [27,28].

In the area of the human breast structure, the studies have been mainly observational, either through imaging (ultrasound) [28–30] or visualization (anatomization) of the 3D ductal system [31–33]. Issues related to lactation and infant suckling mechanism have also been studied by clinicians [34–50]. It is worth emphasizing that the studies of the breast have by and far been biological and clinical in nature, and there is a clear absence of a fundamental biofluid transport study of the breast.

In the area of mathematical modeling of the lactating breast, Mortazavi et al. [51] (authors of the present paper) studied the milk transfer from alveolar sacs through the mammary ducts to the nipple mathematically. They showed that there is an optimal range of bifurcation numbers leading to the easiest milk flow based on the minimum flow resistance. The model formulates certain difficult-to-measure values in breast ductal system (e.g., dimension of alveoli) as a function of easy-to-measure properties such as milk flow properties and macroscopic measurements of the breast. In the area of solid mechanics of the lactating breast, Zoppou et al. [52] developed a mathematical model of the breast teat based on quasi-linear poroelastic theory and studied the relation between tissue deformation and applied suckling pressure.

Prieto et al. [53] investigated the relationship between milk transfer and suckling pressure by recording the suckling pressure and milk transfer during complete suckling episodes. A total of 27 recordings, 13 of which were from a single breast and 14 from both breasts, were evaluated. They observed that milk transfer from the second breast was 58% lower than from the first one; this was associated with a significant decrease in milk transferred per suck or per minute without significant changes in sucking pressure. The data suggest that there is either a change in the maternal physiological response to sucking between the first and second breast or a change in the infant in response to the breast.

Kron and Litt [54] developed an apparatus to measure the infant suckling pressure and milk flow during nutritive suckling. The device was constructed in a way that considered the subatmospheric intra-oral pressure as the only factor in flowing the milk and ignored the effect of mouthing or chewing movement. They applied the physical principles to analyze the macroscopic flow characteristics in this instrument. Due to the analogy between infant's suckling behavior and pulsating pump, the result of this analysis was validated by replacing infant with a calibrated and programmed pump which could generate pressure pulses of different amplitude, repetition, and duration.

Elad et al. [55] explored the physical aspects of infant feeding via ultrasound visualizations of the moving components in the oral cavity and a biophysical model. The dynamic characteristics of tongue motion and nipple movement during breastfeeding were

[1]Corresponding author.

Manuscript received May 26, 2015; final manuscript received October 6, 2016; published online November 30, 2016. Assoc. Editor: Alison Marsden.

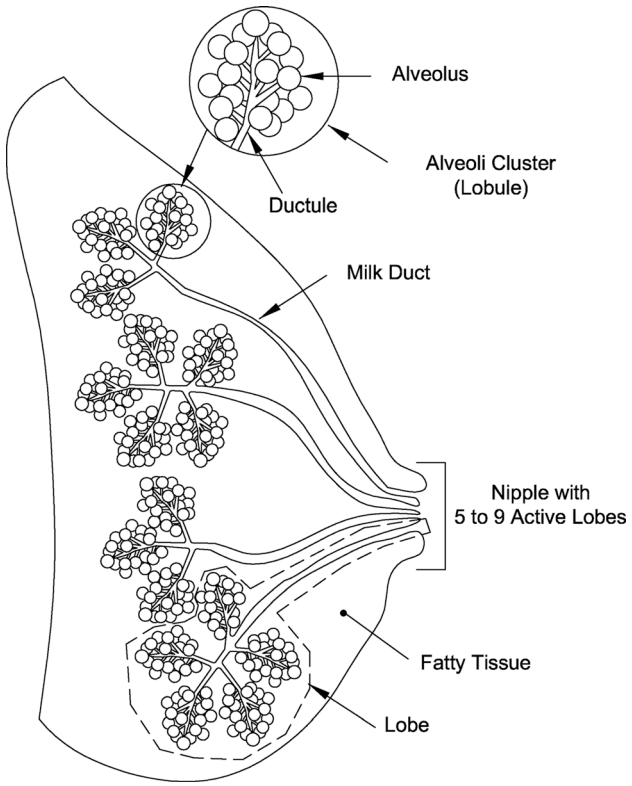

Fig. 1 Anatomy of the lactating breast

studied by computational fluid dynamics modeling. This study assumed a periodic pressure cycling between −20 mmHg and −40 mmHg. They have conducted a CFD modeling of milk flow for duration of one suck on a symmetric geometry of one lobe with two bifurcation levels.

To the best of the authors' knowledge, no computational fluid dynamics study has been attempted until now for the ductal structure of the human breast and its interaction with the boundary conditions driven by the suckling action of an infant for a complete duration of breastfeeding. This paper reports the results of a collaborative effort among lactation specialists and fluid dynamics engineers. The methodology of this study starts with measurements by lactation specialist, yielding a set of precise and statistically representative data on suckling pressure. High-quality clinical data are essential to the integrity of such a study and its practical relevance, since it is known that infants instinctively vary their suckling pressure in a complex manner [48,50]. This data produces useful and dependable boundary conditions for the CFD study.

The CFD itself is dependent on the development of a sound model for the breast ductal system geometry, which is essentially a tree structure starting from the alveoli, whose branches are grouped into lobules and lobes. One of the key contributions of this work is a 3D model of the lactating breast that is simple yet accurate enough, which was produced after several attempts and is briefly described in the sequel. Simulations have been performed using this model and the accurate boundary conditions mentioned above, and the results are described and analyzed.

2 Methods for Clinical Data Collection and CFD Simulation

We begin by highlighting certain useful facts and figures from the biology of the human breast. Subsequently, we concentrate on the task of extracting a biologically representative geometry to be used for the CFD analysis.

The human breast is a dynamic organ that achieves its maturation when a woman experiences pregnancy and childbirth [26]. During pregnancy, the mammary glands and the terminal ductal lobular units enlarge notably in anticipation of lactation. The milk flow system in the lactating breast resembles a tree in which the leaves are the milk glands (alveoli), the grapelike spherical cavity structure (Fig. 1). Milk is produced from the nutrients (including fat, sugar, and protein) and water that are diffused from the adjacent blood stream into the alveoli. A collection of alveoli is called a lobule. Around 20–40 lobules join together to make a lobe [56]. Several works [32,33,57] show that more than 90% of nipple consist of 15–20 lobes, out of which only five to nine are true mammary duct openings (orifices) and the rest are sebaceous glands which change in length from 1 to 4 cm with no connections to the ducts [28,29]. The first branching happens $L_0 = 8 \pm 5.5$ mm from the nipple with the diameter of $D_0 = 1.9 \pm 0.6$ mm [29].

A key part of the CFD modeling and analysis has been to produce a representative geometry in a suitable numerical form for the purposes of CFD analysis. The CFD analysis for other biological organs has a number of precedents in the literature where the relevant analysis has extracted the geometry using various imaging modalities. This has been especially prevalent in the analysis of the lung [58] and kidney [59]. The standard method is to use a high-quality image of the related ductal system, use image processing algorithms to improve the contrast of the image, extract the ductal geometry via image edge extraction methods, and clean up the results via noise removal and homomorphic filtering to ensure continuity of the ducts [60].

The corresponding task for the human breast is significantly more difficult, chiefly because of the fatty tissue in the human breast that produces extremely low contrast with respect to the ducts. The upshot is that the ductal system geometry is not recoverable to a desirable level of detail from any of the existing imaging modalities, including ultrasound or magnetic resonance

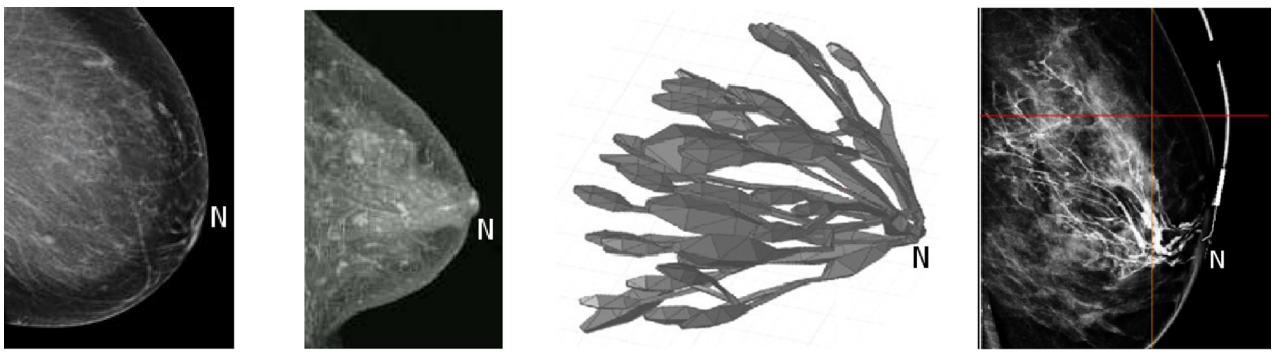

(*a*) (*b*) (*c*) (*d*)

Fig. 2 Comparison of ductal system images (in terms of resolution and accuracy) to produce a representative geometry for CFD simulation purposes: (*a*) ultrasound, (*b*) MRI, (*c*) human body library, and (*d*) ductogram, where "N" stands for nipple

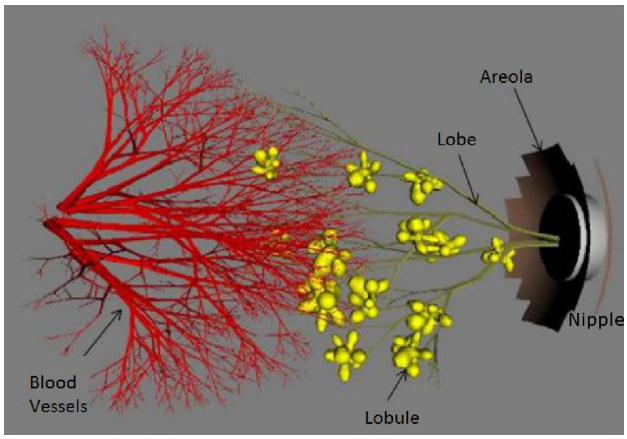

Fig. 3 The breast phantom model being used in this paper for reproducing the geometry model [30]

imaging (Figs. 2(*a*) and 2(*b*)). Ready-made models such as the "human body model" in ANSYS/ANSOFT(HFSS) are simply not sufficiently realistic, for example, the ductal cross sections are square in this model, while they are circular in real life (Fig. 2(*c*)).

Another noteworthy alternative considered by the authors is ductogram/galactogram imaging, a special type of mammogram that injects an X-ray dye into a duct for better visualization. Unfortunately, the ductogram data are not imaged as a volume dataset, and also the ductogram does not produce an image for the entire ductal system at the same time (Fig. 2(*d*)).

To initiate the preliminary study of flow in human ducts, we have used an existing phantom model developed by Baum [61] and validated against the anatomical data. This breast phantom was developed mainly as a ground truth to be able to simulate and evaluate the accuracy of breast imaging modalities and algorithms. Figure 3 portrays the interior of breast phantom (one lobe only) using surface rendering techniques. Tissue includes skin,

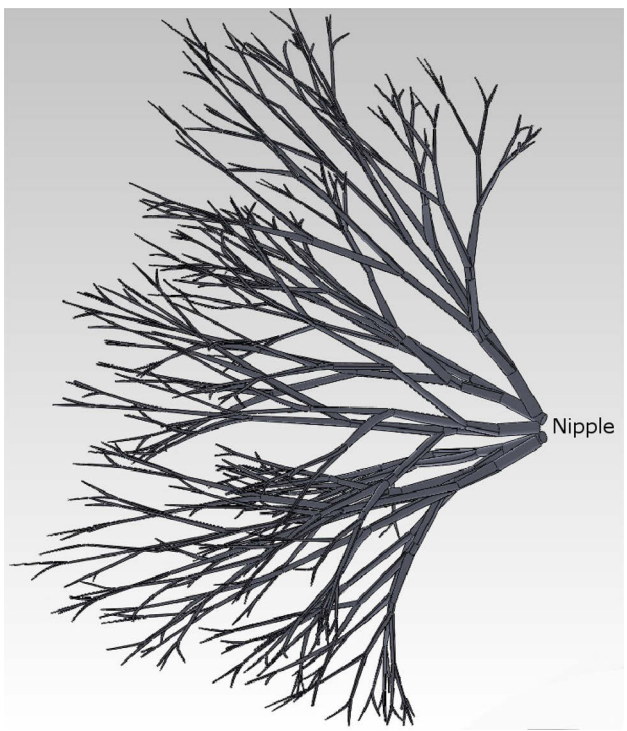

Fig. 4 Three-dimensional visualization of breast ductal branching model based on the phantom model

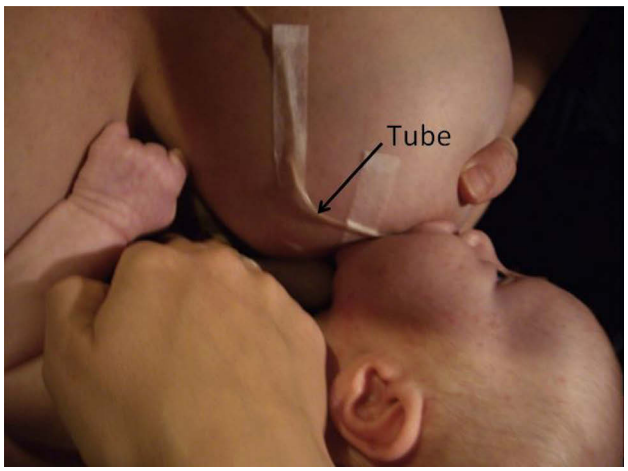

Fig. 5 Pressure measurement of intra-oral cavity during breastfeeding

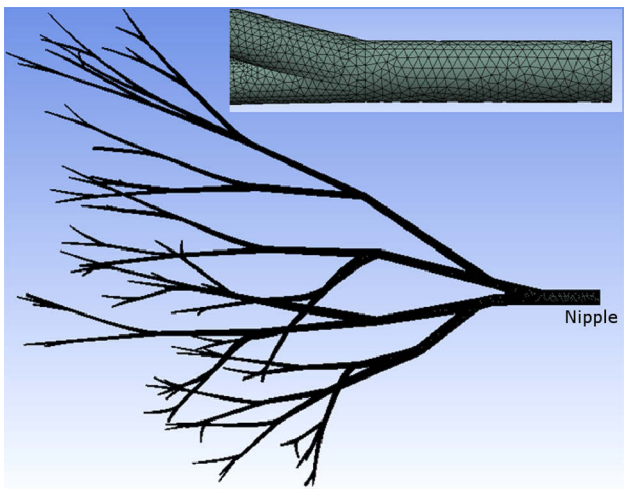

Fig. 6 View of generated mesh of six generations of breast ductal system with 2.52×10^6 elements based on phantom model

areola, lobule, ductal system (up to six generations), and blood. Among these, only the ductal system is chosen for the current study and imported into the CFD software as the geometry base of the model. Considering the fact that breast includes five to nine lobes, Fig. 4 shows a typical image of entire breast ductal system (in the SOLIDWORK software) by multiple copying of one lobe from the phantom model. This ductal system has been used as the final geometry exported in the ANSYS FLUENT software.

Information about boundary conditions (suckling pressure) has been obtained via a close collaboration with clinicians at the University of Western Australia. Suckling pressure and milk intake for 15 infants were obtained through the Child and Adolescent Community Health Center (Oceanic Area Health Service), Perth, Western Australia. The infants were healthy, full term aged 18 ± 6 days (early lactation), with neither any difficulties in breastfeeding nor oral abnormalities. The data included recorded intra-oral vacuum for the entire breastfeeding as well as milk intake measurements.

To collect the pressure data, a small silicone tube (Supplemental Nursing System, Medela AG, Baar, Switzerland) filled with sterile water was used to measure the intra-oral vacuum pressure (Fig. 5). One end of the tube was attached alongside the nipple

(extended 1–2 mm beyond the tip) and the other end was fixed through a silicone tube with the dimension of 650 mm × 4 mm and a three-way tap to a pressure transducer (SP854, Memscap, Bernin, France) with disposable clip-on dome (MLA844, AD Instruments, Castle Hill, Australia). The pressure transducer was synchronized by a customized computerized data collection system called LactaSearch (LactaSearch, Medela AG, Baar, Switzerland), and recorded using the software package DIADEM (version 11.1, National Instruments, Texas, USA, 2009) with a custom-designed program for offline data analysis [46]. Transient pressure profiles $P(t)$ have been derived based on these data collections in periodic form to be used as outlet boundary conditions for the CFD simulation. These axial periodic suckling pressure profiles are written in separate user-defined functions (UDFs) in C++ and interpreted in FLUENT.

During the clinical data collection, at each recording, milk intake is obtained by weighing the infant before and after breastfeeding using an electronic baby weigh scale (Medela AG, Baar, Switzerland, with accuracy ±0.034%). The milk intake (gr) was computed by subtracting the initial weight from the final weight.

Using the commercial ANSYS FLUENT software, the UDF files (boundary conditions) from the clinical data are applied to the developed breast ductal system geometry. The results from the CFD modeling are compared with the clinical data. The suckling pressure is applied to the nipple side of the lobe, and the proximal end (fixed position adjacent to alveoli) is considered to have zero pressure [52,55]. In this study, the walls of the milk ducts are assumed to be rigid with no-slip boundary condition. Both inlet and outlet boundary conditions are applied perpendicular to the inlet (alveoli) and outlet (nipple) cross sections.

The milk is considered as an incompressible Newtonian fluid [62] with approximate density $\rho = 1030\ \mathrm{kg/m^3}$. The clinical data for viscosity measurement indicate that the viscosity of human milk varies greatly during the first few days of lactation (early breastfeeding). The viscosity can be as high as $50 \times 10^{-6}\mathrm{m^2/s}$ in the first day of lactation and falls rapidly as low as to $1.66 \times 10^{-6}\mathrm{m^2/s}$ in the second week of breastfeeding. The viscosity remains in a fairly uniform level after that [63]. Since our pressure (boundary conditions) and milk intake data are related to early lactation, therefore, we have assumed an average value for the viscosity $\nu = 26 \times 10^{-6}\mathrm{m^2/s}$ in the current study. Table 1 shows the physical data considered in the CFD simulation.

Considering the largest value of initial duct diameter (2 mm) [29] and maximum observed milk flow rate (4.8 ml/min) [37,46], the maximum Reynolds number of the milk flow in the conduits will be around Re = 30 which corresponds to laminar flow. Therefore, the milk flow motion in ducts is assumed as unsteady laminar flow. The governing equations of momentum conservation (Navier–Stokes equations) and mass conservation (continuity equation) are solved via CFD simulation for six generations of duct branches in the breast ductal system. Tetrahedral unstructured meshes were used for the interior of the milk ducts with 2.52×10^6 elements (Fig. 6). The problem was first solved with a fairly coarse mesh. After convergence, the solution was improved by refining the mesh (gradient adaption tool), by seeking the locations where a refinement of the mesh would be useful. Using the mesh adaption method, nodes with high-pressure gradients were detected and marked. The grid was refined in the marked region and the procedure was repeated until the pressure solution became mesh independent. Therefore, the resulting mesh was optimal for the flow solution. Thus, the effect of mesh refinement (grid adaption) on the flow solution can be studied without completely regenerating the mesh, and the computational resources are not wasted with unneeded cells [65–67].

Transport equations were discretized by second-order accurate time stepping and a second-order accurate discretization scheme. The semi-implicit method for pressure-linked equations algorithm was applied to evaluate the pressure–velocity coupling. The laminar solution of the flow field was assumed to be converged when

Table 1 The value of various physical parameters based on direct measurements

Parameter	Symbol	Value	Reference
Number of lobules per lobe	a	20–40	[56]
Number of active lobes in each breast	b	5–9	[26]
Initial duct length	L_0	8 ± 5 mm	[29]
Initial duct diameter	D_0	1.9 ± 0.6 mm	[29]
Milk density	ρ	1030 ($\mathrm{kg/m^3}$)	[64]
Milk viscosity (early lactation)	ν	1.66–51.90 $\times 10^{-6}$ ($\mathrm{m^2/s}$)	[63]

Table 2 Representative of time-step accuracy

Δt (s)	$\dot{V}$ (ml/s) at instance $t = 502$ s
0.5	0.0638
0.25	0.0406
0.125	0.0191
0.0625	0.0170
0.03125	0.0166

Table 3 Clinical experiment on 15 infants

				Milk intake		
Infant label	Average pressure (kPa)	Feeding duration (s)	Number of cycles	(ml)	(ml/s)	(ml/cycle)
Infant-A	−14.07±−7.19	501	386	135	0.27	0.34
Infant-B	−13.82±−7.38	856	553	68	0.08	0.12
Infant-C	−12.14±−8.49	702	571	112	0.16	0.19
Infant-D	−4.49±−1.82	737	619	74	0.1	0.12
Infant-E	−6.81±−4.66	613	468	52	0.084	0.11
Infant-F	−16.54±−8.43	394	389	108	0.27	0.28
Infant-G	−7.08±−4.17	1007	367	30	0.05	0.08
Infant-H	−9.31±5.93	939	561	76	0.081	0.14
Infant-I	−12.93±−3.95	1033	538	58	0.056	0.11
Infant-J	−6.99±−3.91	565	677	78	0.138	0.12
Infant-K	−8.59±−3.50	953	437	100	0.104	0.23
Infant-L	−6.25±−5.88	802	757	166	0.21	0.22
Infant-M	−9.99±−4.23	409	148	130	0.31	0.88
Infant-N	−8.172±−5.72	445	117	92	0.206	0.79
Infant-O	−14.37±−9.62	204	99	130	0.21	1.31
Avg. value	−10.10±−5.66	674.51	455.2	93.93	0.18	0.34

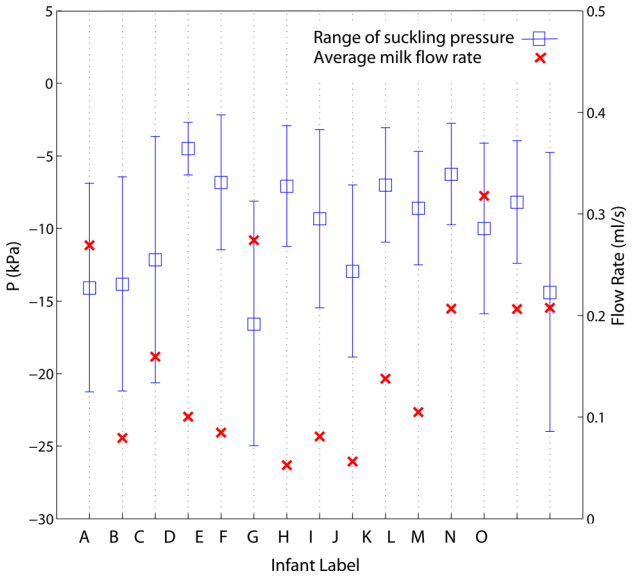

Fig. 7 Suckling pressure range and the average milk flow rate for each infant based on the clinical measurements

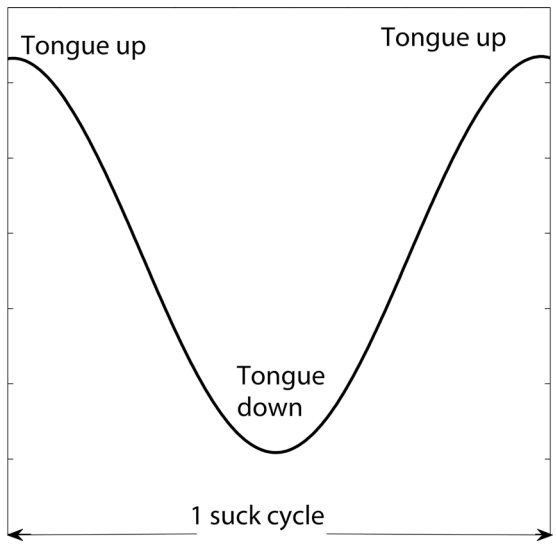

Fig. 8 Representative of a suck cycle versus tongue position

the continuity and momentum equations residuals reduced to less than 10^{-6}. Comprehensive convergence tests were done to investigate the time-step size. Table 2 shows the effect of time interval sizes in the average milk flow rate ($\dot{V}$) obtained by the CFD simulation, indicating that the time step of $\Delta t = 0.0625$ s is a suitable value. The number of iterations per time step was large enough to meet the convergence criterion.

After completing the simulation model including the geometry and flow domain, establishing the boundary and initial conditions, generating the grids, and simulation strategy settlement, the results for milk intake and milk flow rate at each stage of breastfeeding are compared against the comprehensive clinical data.

3 Results and Discussion

Figure 7 represents the average maximum (baseline) and minimum (peak) pressure for all 15 infants along with their related milk intake value. The results from clinical data for average suckling pressure, feeding duration, number of cycles, total milk intake, average milk flow rate, and milk flow per cycle are shown in Table 3. In the last row of the table, the average among all 15 infants is listed. Looking at these clinical data, one can observe that largest milk flow rate is not related to the infant with maximum pressure or longest duration of breastfeeding. It is obtained from the results that in a suck cycle (Fig. 8), vacuum pressure is not the only reason for milk removal from the breast and other parameters such as suckling, swallowing, and breathing interruptions may be involved. This is in contrast with several previous studies that claim vacuum plays an important role in the removal of milk from the breast [53,55].

Figure 9 presents a sample of graph (infant-A) for the recorded suckling pressure. As shown, the vacuum pressure is not applied uniformly with the same period and number of sucks for the entire breastfeeding duration (8–15 min), but rather changes with the infant's patterns of nutritive and non-nutritive sucking defined by the presence or absence of milk. Also, the milk ejection happens early in the breastfeeding and persists for a short period of time to keep an internal pressure within the ductal system, providing the continuous progress of milk into the nipple. Figure 10 shows a clear presentation of transient pressure profile $P(t)$ during each phase of the breastfeeding for infant-A.

The related equation $P(t)$ in each phase is in a periodic form (Eq. (1)). The correlation is derived as a function of recorded data of average maximum (baseline) and minimum (peak) pressure, number of sucks per burst, burst duration, interburst duration, and intersuck duration for each section of burst and pause, nutritive and non-nutritive phase (Fig. 11).

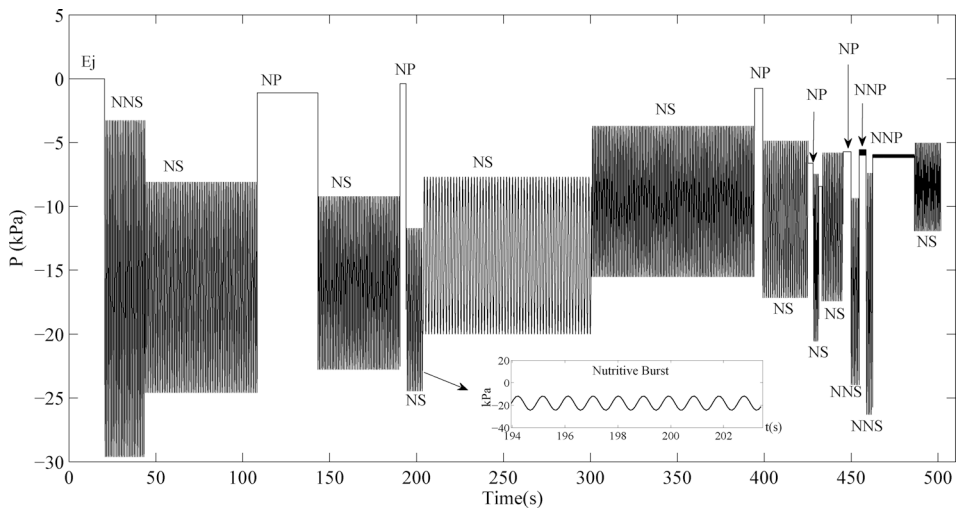

Fig. 9 Various phases of suckling by one of the infants (infant-A): Ej (ejection), NNS (non-nutritive burst), NS (nutritive burst), NP (nutritive pause), and NNP (non-nutritive pause)

According to these clinical data, the outlet pressure profile is approximately sinusoidal in each of the subintervals, e.g., nutritive and non-nutritive suckling phases. Therefore, we use regression to match the measured values in each interval to a sinusoid of the following form:

$$P(t) = A \sin^2(\xi t) + B \tag{1}$$

where $(t, P(t))$ are the experimental data points, and (ξ), (A), and (B) are the values determined by the regression.

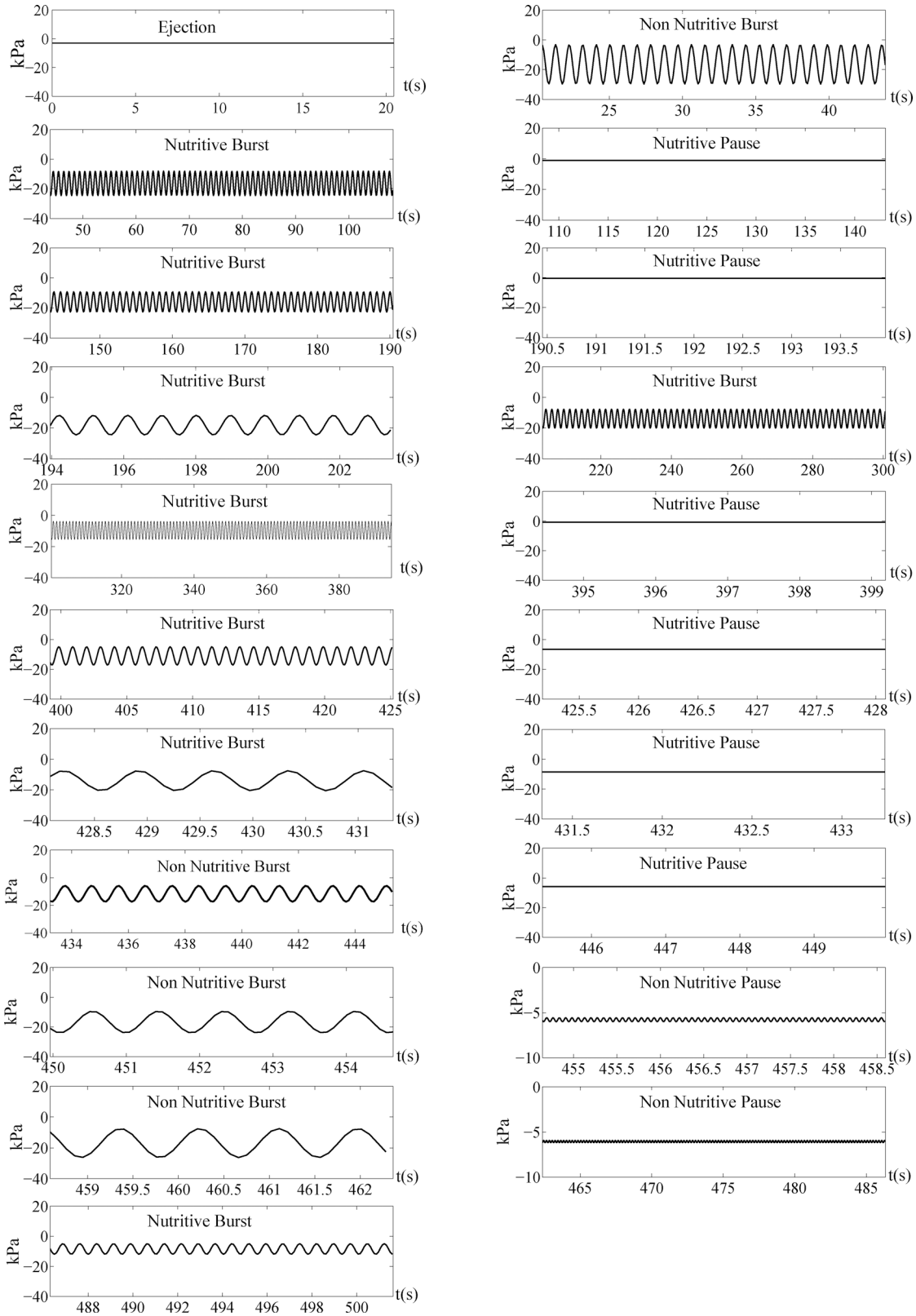

Fig. 10 Detailed pressure profiles for 21 stages of breastfeeding by infant-A, $0 \le t \le 502$ s

Table 4 Pressure profiles for outlet boundary condition (infant-A)

Time (s)	Pressure profile (kPa)
$t < 20.44$	$P(t) = -2.7$ to -3.4
$20.44 < t < 43.85$	$P(t) = -26.3230\sin^2(3.4t) - 3.2744$
$43.85 < t < 108.33$	$P(t) = -16.4680\sin^2(3.2t) - 8.1167$
$108.33 < t < 143.13$	$P(t) = -1.1039$
$143.13 < t < 190.45$	$P(t) = -13.5200\sin^2(3.5t) - 9.2446$
$190.45 < t < 193.96$	$P(t) = -0.3773$
$193.96 < t < 203.4800$	$P(t) = -12.7430\sin^2(3.3t) - 11.7220$
$203.4800 < t < 300.64$	$P(t) = -12.2670\sin^2(1.9t) - 7.7221$
$300.64 < t < 394.4300$	$P(t) = -11.7910\sin^2(3.5t) - 3.7224$
$394.43 < t < 399.19$	$P(t) = -0.7466$
$399.19 < t < 425.19$	$P(t) = -12.2720\sin^2(3.0t) - 4.8876$
$425.19 < t < 428.08$	$P(t) = -6.6181$
$428.08 < t < 431.33$	$P(t) = -13.0620\sin^2(4.4t) - 7.4861$
$431.33 < t < 433.24$	$P(t) = -8.4580$
$433.24 < t < 445.34$	$P(t) = -11.6100\sin^2(3.3t) - 5.8089$
$445.34 < t < 449.96$	$P(t) = -5.7262$
$449.96 < t < 454.64$	$P(t) = -14.5970\sin^2(3.5t) - 9.3699$
$454.64 < t < 458.59$	$P(t) = -0.4479\sin^2(43.1t) - 6.0048$
$458.59 < t < 462.36$	$P(t) = -118.8880\sin^2(3.6t) - 7.4141$
$462.36 < t < 486.34$	$P(t) = -0.2426\sin^2(15.7t) - 6.1782$
$486.34 < t < 501.6300$	$P(t) = -6.8728\sin^2(4.1t) - 5.0449$

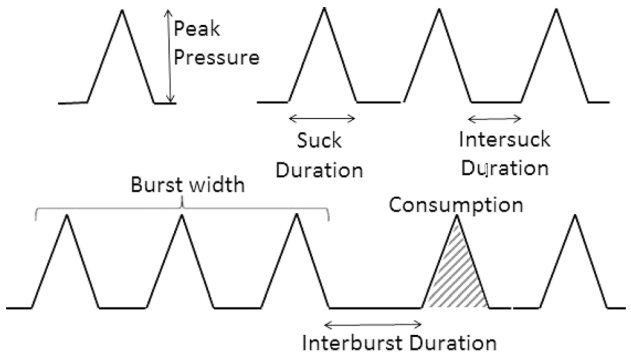

Fig. 11 Representative of burst, interburst, suck, and intersuck durations

Both (A, B) are negative (suction), (A) is the difference between baseline and peak pressure, (B) is the maximum pressure (because $A \leq 0$), and (ξ) is the frequency of the pressure profile. Frequency of the infant suckling (ξ) is defined as the ratio of number of sucking per burst duration. A set of consecutive periodic functions of the form given in Eq. (1) will constitute the boundary conditions. It is useful to recall that this set of functions is representative of the natural rhythm suckling that includes sucking, pausing, and breathing, and involves a combination of the actions of tongue and jaw movements. Table 4 shows the related derived equations of vacuum pressure profiles for infant-A in each phase of breastfeeding.

Applying these periodic equations as outlet boundary conditions for nipple, Figs. 12 and 13 show the milk intake in each time interval and the average of milk flow rate in each stage of suckling, respectively. As observed in both figures, major milk flow occurs in the first stages of infant suckling, while less milk flow is observed in later stages. These results are in line with our clinical measurements on infant-A in which almost 50% of the total milk intake occurs in the first 2 min of suckling and 80–90% by first 4 min. This phenomenon was observed by clinical data and monitoring the milk flow rate during a full breastfeeding duration by Woolridge et al. [43] as well.

Also, comparing the milk flow rate in each stage and its related absolute vacuum pressure in the same stage shows that the maximum flow rate (the most productive stage) is not related to the maximum vacuum pressure or vice versa, the minimum milk flow rate does not correspond to the stage with the maximum pressure value. The milk intake was not related to peak or baseline vacuum indicating other factors influence the intake of milk of the infant such as appetite and fullness of the breast.

Having the number of suck cycles and milk flow rate in each stage, the value of milk flow rate per suckling cycle is obtained via CFD simulation in each stage. The results show that the milk flow rate per cycle is decreasing from 0.4 ml/cycle in the beginning stages to 0.2 ml/cycle in the latest stages of breastfeeding. This phenomenon was observed in the clinical experiments by Woolridge [43] and Pierto et al. [53] as well. This progressive reduction in intake volume per suck and also the increase of pause burst of sucking in the last stages of breastfeeding contribute to the curtailment of intake during the breastfeeding. Table 5 gives an overview of the current study and comparison with previous related studies.

From the CFD simulation, the accumulative milk intake during the total duration of breastfeeding for five lobes (infant-A) is 250 (ml) which is 1.85 times higher than the clinical measurements for

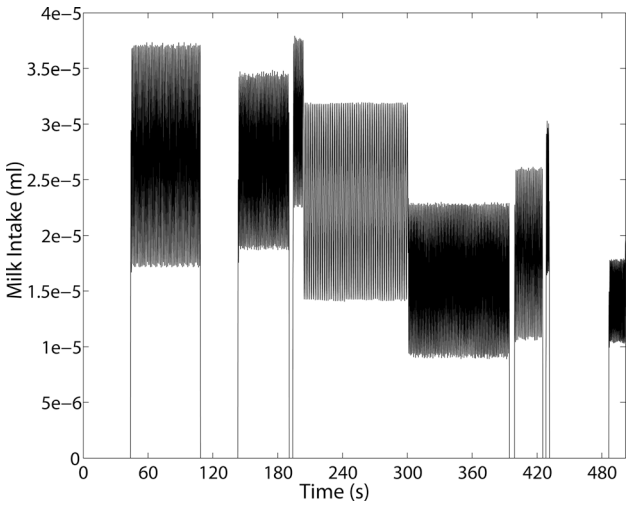

Fig. 12 Results from the CFD simulation: instantaneous milk intake (ml) during the total duration of breastfeeding

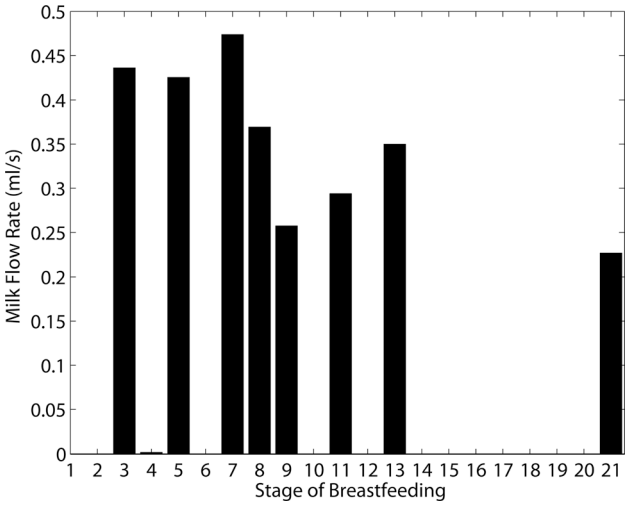

Fig. 13 Results from the CFD simulation: average value of milk flow rate (ml/s) in different stages of suckling (shown in Fig. 10)

Table 5 Key specifications and results from our study in comparison with past work

	Experimental study			CFD simulation	
	Woolridge et al. [34]	Prieto et al. [53]	Current study	Elad et al. [55]	Current study
Type of investigation	Clinical measurement (average values)			CFD modeling	
Number of infants	6	17	15	1	infant-A (out of 15)
Geometry	N/A	N/A	N/A	Symmetric branching (two generations)	Phantom model (six generations)
Duration (min)	9 ± 6	7 ± 0.7	14.49 ± 4.02	0.021 (0.64 s/cycle)	8.36
Number of suck cycles	55	364 ± 183	428 ± 329	2	386
Mean pressure (kPa)	N/A	-6.67 ± 0.76	-10.10 ± 5.66	-4 ± 1.33 (-20 to -40 mmHg)	-14.07 ± 7.19
Milk intake (ml)	34.2 (left breast) and 26.2 (right breast)	56 ± 7.8	93.1 ± 32.4	N/A	250 (for five lobes)
Milk intake (ml/cycle)	0.075 ± 0.065	0.17 ± 0.15	0.68 ± 0.59	≈ 0.11	0.64

that specific infant (135 ml). A similar result was obtained by Elad et al. [55], who found three times more milk flow intake via a solid geometry with two bifurcation levels. The relationship of the simulation and clinical data is certainly noteworthy, leading to the following observation. The flow resistance increases substantially with increasing number of bifurcations, a fact that is not only intuitive but also mathematically verified in Ref. [55]. The current work uses a model with six bifurcation levels, producing milk flow within a factor of 1.8 of clinical data. Elad et al. [55] used a symmetric model with only two bifurcation level, experiencing a larger discrepancy with clinical data. The number of bifurcations occurring in nature is variable and not perfectly known; however, it has been mathematically estimated in Ref. [51] to be on the order of $n = 20$–40. It is expected that simulation involving more bifurcations in the future can reduce the gap to clinical data. In addition, other factors also contribute to the resistance to milk flow. These factors include deformed region of the areola–nipple, reduction of ducts cross-sectional areas due to squeezing of the nipple, and elasticity of the tissue. More sophisticated future simulations via modeling of these effects can shed further light on the mechanics of milk flow and produce closer results to clinical data.

4 Conclusion

A CFD modeling of milk flow through branching ducts in the human breast was presented. The commercial ANSYS FLUENT software was used for numerical simulation. The geometry was extracted from a phantom model, and the boundary conditions, mainly infant vacuum pressure, were obtained from the clinical measurements on a group of infants.

The results for milk intake from the CFD simulation and clinical data were compared. The clinical data show that suckling action does not occur with constant suckling rate but changes in a rhythmic manner for infants. Both the clinical and CFD simulation show that the maximum milk flow rate is not related to the largest vacuum pressure or longest feeding duration. The results from the simulation modeling indicate that the majority of milk intake is during the first stages of breastfeeding, almost 50% during the first 2 min, and around 80–90% during the first 4 min. This has been validated with our clinical measurements.

The analysis and comparison of the gap between the simulation and clinical data from several studies show that the branching ductal system and the forces from infant jaw movement and oral cavity are important factors in milk flow, which have to date been incorporated into analysis only up to a certain point. In addition, several other factors may also contribute to milk flow, including the deformed region of the areola–nipple, reduction of ducts cross-sectional areas due to squeezing of the nipple, and elasticity of the tissue. These factors have to date not been incorporated into formal studies of milk flow, and more work is needed to reveal the relative importance of their role.

Acknowledgment

The authors acknowledge the financial support from the National Science Foundation (CAREER) Grant No. 1454334 and also Dr. Karl G. Baum (Biomedical and Materials Multimodal Imaging Laboratory, Rochester Institute of Technology, Chester F. Carlson Center for Imaging Science) for providing the 3D phantom model of the human breast.

Nomenclature

a = number of lobules in each lobe
b = number of active mammary ducts
D_0 = initial duct diameter (mm)
L_0 = initial duct length (mm)
n = number of bifurcations
P = pressure (Pa)
Re = Reynolds number
t = time (s)
$\mathbf{v}$ = velocity (m/s)
$\dot{V}$ = volumetric flow rate (ml/s)
Δt = time interval (s)

Greek Symbols

ν = kinematic viscosity (m^2/s)
ξ = frequency ($1/s$)
ρ = density (kg/m^3)

References

[1] Lei, M., Giddens, D., Jones, S., Loth, F., and Bassiouny, H., 2001, "Pulsatile Flow in an End-to-Side Vascular Graft Model: Comparison of Computations With Experimental Data," ASME J. Biomech. Eng., **123**(1), pp. 80–87.
[2] Wang, D. H., Makaroun, M., Webster, M. W., and Vorp, D. A., 2001, "Mechanical Properties and Microstructure of Intraluminal Thrombus From Abdominal Aortic Aneurysm," ASME J. Biomech. Eng., **123**(6), pp. 536–539.
[3] Rayz, V. L., Lawton, M. T., Martin, A. J., Young, W. L., and Saloner, D., 2008, "Numerical Simulation of Pre- and Postsurgical Flow in a Giant Basilar Aneurysm," ASME J. Biomech. Eng., **130**(2), p. 021004.
[4] Kulish, V. V., Lage, J. L., Hsia, C. C., and Johnson, R. L., 2002, "Three-Dimensional, Unsteady Simulation of Alveolar Respiration," ASME J. Biomech. Eng., **124**(5), pp. 609–616.
[5] Liu, Y., So, R., and Zhang, C., 2002, "Modeling the Bifurcating Flow in a Human Lung Airway," J. Biomech., **35**(4), pp. 465–473.
[6] Zhao, Y., Brunskill, C., and Lieber, B., 1997, "Inspiratory and Expiratory Steady Flow Analysis in a Model Symmetrically Bifurcating Airway," ASME J. Biomech. Eng., **119**(1), pp. 52–58.
[7] Allen, G., Shortall, B., Gemci, T., Corcoran, T., and Chigier, N., 2004, "Computational Simulations of Airflow in an In Vitro Model of the Pediatric Upper Airways," ASME J. Biomech. Eng., **126**(5), pp. 604–613.
[8] Keyhani, K., Scherer, P., and Mozell, M., 1995, "Numerical Simulation of Airflow in the Human Nasal Cavity," ASME J. Biomech. Eng., **117**(4), pp. 429–441.
[9] Shome, B., Wang, L., Santare, M., Prasad, A., Szeri, A., and Roberts, D., 1998, "Modeling of Airflow in the Pharynx With Application to Sleep Apnea," ASME J. Biomech. Eng., **120**(3), pp. 416–422.

[10] Mylavarapu, G., Murugappan, S., Mihaescu, M., Kalra, M., Khosla, S., and Gutmark, E., 2009, "Validation of Computational Fluid Dynamics Methodology Used for Human Upper Airway Flow Simulations," J. Biomech., **42**(10), pp. 1553–1559.
[11] Lee, C. Y., and Rubinsky, B., 1989, "A Multi-Dimensional Model of Momentum and Mass Transfer in the Liver," Int. J. Heat Mass Transfer, **32**(12), pp. 2421–2434.
[12] Debbaut, C., Vierendeels, J., Casteleyn, C., Cornillie, P., Van Loo, D., Simoens, P., Van Hoorebeke, L., Monbaliu, D., and Segers, P., 2012, "Perfusion Characteristics of the Human Hepatic Microcirculation Based on Three-Dimensional Reconstructions and Computational Fluid Dynamic Analysis," ASME J. Biomech. Eng., **134**(1), p. 011003.
[13] Bonfiglio, A., Leungchavaphongse, K., Repetto, R., and Siggers, J. H., 2010, "Mathematical Modeling of the Circulation in the Liver Lobule," ASME J. Biomech. Eng., **132**(11), p. 111011.
[14] Debbaut, C., Vierendeels, J., Siggers, J. H., Repetto, R., Monbaliu, D., and Segers, P., 2012, "A 3D Porous Media Liver Lobule Model: The Importance of Vascular Septa and Anisotropic Permeability for Homogeneous Perfusion," Comput. Methods Biomech. Biomed. Eng., **17**(12), pp. 1295–1310.
[15] Rani, H., Sheu, T. W., Chang, T., and Liang, P., 2006, "Numerical Investigation of Non-Newtonian Microcirculatory Blood Flow in Hepatic Lobule," J. Biomech., **39**(3), pp. 551–563.
[16] Loth, F., Yardimci, M. A., and Alperin, N., 2001, "Hydrodynamic Modeling of Cerebrospinal Fluid Motion Within the Spinal Cavity," ASME J. Biomech. Eng., **123**(1), pp. 71–79.
[17] Linninger, A. A., Xenos, M., Zhu, D. C., Somayaji, M. R., Kondapalli, S., and Penn, R. D., 2007, "Cerebrospinal Fluid Flow in the Normal and Hydrocephalic Human Brain," IEEE Trans. Biomed. Eng., **54**(2), pp. 291–302.
[18] Beard, D. A., and Bassingthwaighte, J. B., 2001, "Modeling Advection and Diffusion of Oxygen in Complex Vascular Networks," Ann. Biomed. Eng., **29**(4), pp. 298–310.
[19] Moore, S., David, T., Chase, J., Arnold, J., and Fink, J., 2006, "3D Models of Blood Flow in the Cerebral Vasculature," J. Biomech., **39**(8), pp. 1454–1463.
[20] Lee, B. K., 2011, "Computational Fluid Dynamics in Cardiovascular Disease," Korean Circ. J., **41**(8), pp. 423–430.
[21] Schirmer, C. M., and Malek, A. M., 2007, "Prediction of Complex Flow Patterns in Intracranial Atherosclerotic Disease Using Computational Fluid Dynamics," Neurosurgery, **61**(4), pp. 842–852.
[22] Brebbia, C. A., 2011, *Modelling in Medicine and Biology*, WIT Press, Ashurst, Southhampton, UK.
[23] Sotiropoulos, F., 2012, "Computational Fluid Dynamics for Medical Device Design and Evaluation: Are We There Yet?," Cardiovasc. Eng. Technol., **3**(2), pp. 137–138.
[24] De Leval, M. R., and Dubini, G., 1996, "Use of Computational Fluid Dynamics in the Design of Surgical Procedures: Application to the Study of Competitive Flows in Cavopulmonary Connections," J. Thorac. Cardiovasc. Surg., **111**(3), pp. 502–513.
[25] Liu, Y., and Zheng, J., 2011, "Research Progress of Computational Fluid Dynamics in Surgical Approach Simulation for Congenital Heart Disease," J. Shanghai Jiaotong Univ. (Med. Sci.), **31**(9), pp. 1325–1327.
[26] Geddes, D. T., 2007, "Inside the Lactating Breast: The Latest Anatomy Research," J. Midwifery Women's Health, **52**(6), pp. 556–563.
[27] Riordan, J., and Wambach, K., 2010, *Breastfeeding and Human Lactation*, Jones & Bartlett Learning, Burlington, MA.
[28] Love, S. M., and Barsky, S. H., 2004, "Anatomy of the Nipple and Breast Ducts Revisited," Cancer, **101**(9), pp. 1947–1957.
[29] Ramsay, D., Kent, J., Hartmann, R., and Hartmann, P., 2005, "Anatomy of the Lactating Human Breast Redefined With Ultrasound Imaging," J. Anat., **206**(6), pp. 525–534.
[30] Baum, K. G., McNamara, K., and Helguera, M., 2008, "Design of a Multiple Component Geometric Breast Phantom," Proc. SPIE, **6913**, p. 69134H.
[31] Cooper, A. P., 1840, *On the Anatomy of the Breast*, Longman, Rees, Orme, Brown, and Green, London.
[32] Going, J. J., and Moffat, D. F., 2004, "Escaping From Flatland: Clinical and Biological Aspects of Human Mammary Duct Anatomy in Three Dimensions," Pathology, **203**(1), pp. 538–544.
[33] Ohtake, T., Kimijima, I., Fukushima, T., Yasuda, M., Sekikawa, K., Takenoshita, S., and Abe, R., 2001, "Computer-Assisted Complete Three-Dimensional Reconstruction of the Mammary Ductal/Lobular Systems," Cancer, **91**(12), pp. 2263–2272.
[34] Woolridge, M., Baum, J., and Drewett, R., 1982, "Individual Patterns of Milk Intake During Breast-Feeding," Early Hum. Dev., **7**(3), pp. 265–272.
[35] McClellan, H., Geddes, D., Kent, J., Garbin, C., Mitoulas, L., and Hartmann, P., 2008, "Infants of Mothers With Persistent Nipple Pain Exert Strong Sucking Vacuums," Acta Paediatr., **97**(9), pp. 1205–1209.
[36] Eishima, K., 1991, "The Analysis of Sucking Behaviour in Newborn Infants," Early Hum. Dev., **27**(3), pp. 163–173.
[37] Geddes, D. T., Kent, J. C., Mitoulas, L. R., and Hartmann, P. E., 2008, "Tongue Movement and Intra-Oral Vacuum in Breastfeeding Infants," Early Hum. Dev., **84**(7), pp. 471–477.
[38] Medoff-Cooper, B., Bilker, W., and Kaplan, J. M., 2010, "Sucking Patterns and Behavioral State in 1- and 2-Day-Old Full-Term Infants," J. Obstet. Gynecol. Neonat. Nurs., **39**(5), pp. 519–524.
[39] Nowak, A. J., Smith, W. L., and Erenberg, A., 1994, "Imaging Evaluation of Artificial Nipples During Bottle Feeding," Arch. Pediatr. Adolesc. Med., **148**(1), pp. 40–42.
[40] Woolridge, M., Baum, J., and Drewett, R., 1980, "Effect of a Traditional and of a New Nipple Shield on Sucking Patterns and Milk Flow," Early Hum. Dev., **4**(4), pp. 357–364.
[41] Lucas, A., Lucas, P. J., and Baum, J. D., 1980, "The Nipple-Shield Sampling System: A Device for Measuring the Dietary Intake of Breast-Fed Infants," Early Hum. Dev., **4**(4), pp. 365–372.
[42] Drewett, R., and Woolridge, M., 1979, "Sucking Patterns of Human Babies on the Breast," Early Hum. Dev., **3**(4), pp. 315–320.
[43] Woolridge, M. W., 1986, "The Anatomy of Infant Sucking," Midwifery, **2**(4), pp. 164–171.
[44] Koenig, J., Davies, A., and Thach, B., 1990, "Coordination of Breathing, Sucking, and Swallowing During Bottle Feedings in Human Infants," J. Appl. Physiol., **69**(5), pp. 1623–1629.
[45] Geddes, D. T., Langton, D. B., Gollow, I., Jacobs, L. A., Hartmann, P. E., and Simmer, K., 2008, "Frenulotomy for Breastfeeding Infants With Ankyloglossia: Effect on Milk Removal and Sucking Mechanism as Imaged by Ultrasound," Pediatrics, **122**(1), pp. e188–e194.
[46] Sakalidis, V. S., Kent, J. C., Garbin, C. P., Hepworth, A. R., Hartmann, P. E., and Geddes, D. T., 2013, "Longitudinal Changes in Suck-Swallow-Breathe, Oxygen Saturation, and Heart Rate Patterns in Term Breastfeeding Infants," J. Hum. Lactation, **29**(2), pp. 236–245.
[47] Kent, J. C., Ramsay, D. T., Doherty, D., Larsson, M., and Hartmann, P. E., 2003, "Response of Breasts to Different Stimulation Patterns of an Electric Breast Pump," J. Hum. Lactation, **19**(2), pp. 179–186.
[48] Ramsay, D. T., Mitoulas, L. R., Kent, J. C., Cregan, M. D., Doherty, D. A., Larsson, M., and Hartmann, P. E., 2006, "Milk Flow Rates Can Be Used to Identify and Investigate Milk Ejection in Women Expressing Breast Milk Using an Electric Breast Pump," Breastfeed. Med., **1**(1), pp. 14–23.
[49] Kent, J. C., Mitoulas, L. R., Cregan, M. D., Geddes, D. T., Larsson, M., Doherty, D. A., and Hartmann, P. E., 2008, "Importance of Vacuum for Breast Milk Expression," Breastfeed. Med., **3**(1), pp. 11–19.
[50] Ramsay, D. T., Kent, J. C., Owens, R. A., and Hartmann, P. E., 2004, "Ultrasound Imaging of Milk Ejection in the Breast of Lactating Women," Pediatrics, **113**(2), pp. 361–367.
[51] Mortazavi, N., Geddes, D., and Haasanipour, F., 2015, "Mathematical Modeling of Mammary Ducts in Lactating Human Females," ASME J. Biomech. Eng., **137**(7), pp. 071009–071009-8.
[52] Zoppou, C., Barry, S. I., and Mercer, G. N., 1997, "Dynamics of Human Milk Extraction: A Comparative Study of Breast Feeding and Breast Pumping," Bull. Math. Biol., **59**(5), pp. 953–973.
[53] Prieto, C., Cárdenas, H., Salvatierra, A., Boza, C., Montes, C., and Croxatto, H., 1996, "Sucking Pressure and Its Relationship to Milk Transfer During Breastfeeding in Humans," J. Reprod. Fertil., **108**(1), pp. 69–74.
[54] Kron, R., and Litt, M., 1971, "Fluid Mechanics of Nutritive Sucking Behaviour: The Suckling Infant's Oral Apparatus Analysed as a Hydraulic Pump," Med. Biol. Eng., **9**(1), pp. 45–60.
[55] Elad, D., Kozlovsky, P., Blum, O., Laine, A. F., Po, M. J., Botzer, E., Dollberg, S., Zelicovich, M., and Sira, L. B., 2014, "Biomechanics of Milk Extraction During Breast-Feeding," Proc. Natl. Acad. Sci. U.S.A., **111**(14), pp. 5230–5235.
[56] Sohn, C., Blohmer, J. U., and Hamper, U., 1999, *Breast Ultrasound: A Systematic Approach to Technique and Image Interpretation*, Thieme, Stuttgart, Germany.
[57] Moffat, D., and Going, J., 1996, "Three Dimensional Anatomy of Complete Duct Systems in Human Breast: Pathological and Developmental Implications," J. Clin. Pathol., **49**(1), pp. 48–52.
[58] De Backer, L. A., Vos, W., De Backer, J., Van Holsbeke, C., Vinchurkar, S., and De Backer, W., 2012, "The Acute Effect of Budesonide/Formoterol in COPD: A Multi-Slice Computed Tomography and Lung Function Study," Eur. Respir. J., **40**(2), pp. 298–305.
[59] Plainfosse, M., Calonge, V. M., Beyloune-Mainardi, C., Glotz, D., and Duboust, A., 1992, "Vascular Complications in the Adult Kidney Transplant Recipient," J. Clin. Ultrasound, **20**(8), pp. 517–527.
[60] Canny, J., 1986, "A Computational Approach to Edge Detection," IEEE Trans. Pattern Anal. Mach. Intell., **8**(6), pp. 679–698.
[61] Baum, K. G., 2008, *Multimodal Breast Imaging: Registration, Visualization, and Image Synthesis*, PhD Dissertation, Rochester Institute of Technology, Rochester, NY.
[62] Almeida, M. B., Almeida, J. A., Moreira, M. E., and Novak, F. R., 2011, "Adequacy of Human Milk Viscosity to Respond to Infants With Dysphagia: Experimental Study," J. Appl. Oral Sci., **19**(6), pp. 554–559.
[63] Waller, H., Aschaffenburg, R., and Grant, M. W., 1941, "The Viscosity, Protein Distribution, and Gold Number' of the Antenatal and Postnatal Secretions of the Human Mammary Gland," Biochem. J., **35**(3), pp. 272–282.
[64] Neville, M. C., Keller, R., Seacat, J., Lutes, V., Neifert, M., Casey, C., Allen, J., and Archer, P., 1988, "Studies in Human Lactation: Milk Volumes in Lactating Women During the Onset of Lactation and Full Lactation," Am. J. Clin. Nutr., **48**(6), pp. 1375–1386.
[65] Wen, J., Inthavong, K., Tu, J., and Wang, S., 2008, "Numerical Simulations for Detailed Airflow Dynamics in a Human Nasal Cavity," Respir. Physiol. Neurobiol., **161**(2), pp. 125–135.
[66] Ma, B., and Lutchen, K. R., 2009, "CFD Simulation of Aerosol Deposition in an Anatomically Based Human Large–Medium Airway Model," Ann. Biomed. Eng., **37**(2), pp. 271–285.
[67] ANSYS, 2009, "ANSYS FLUENT 12.0 Tutorial Guide," ANSYS, Inc., Canonsburg, PA.